doi:10.20944/preprints201711.0192.v1

Article

Filter selection for optimizing spectral sensitivity of broadband multispectral camera based on maximum linear independence

Sui-Xian Li[1]*, Da-Qi Xu[2], Li-Yan Zhang[3] and Jun Lin[2]

[1] Binzhou University, Binzhou, Shandong, China, 256600;leesx_72@163.com
[2] China Centre for Resource Satellite Data and Application, Beijing, China,100094; xudaqi@spacechina.com
[3] College of Resources Environment and Tourism, Capital Normal University, Beijing, China, 100048 zhangliyan010@126.com
* Correspondence: leesx_72@163.com; Tel.: +86-18600890892

Abstract: Previous research has shown that the effectiveness of selecting filter set from a large set of commercial broadband filters by vector analyzing method based on maximum linear independence (MLI). However, the traditional MLI is suboptimal due to predefining the first filter of the selected filter set being the maximum ℓ2 norm among all those of the filters. An exhaustive imaging simulation is conducted to investigate the features of the most competent filter set. In the simulation, every filter in a subset of all the filters is selected serving as the first filter in turn. From the results of the simulation, we found there are remarkable characteristics for the most competent filter set. Besides smaller condition number, the geometric features of the best-performed filter set comprise the distinct peak of the transmittance of the first filter, the generally uniform distributing of the peaks of the transmittance curve of the filters, the substantial overlapping of the transmittance curves with those of the adjacent filer sets. Therefore, the best-performed filter sets can be decided intuitively by simple vector analyzing and just a few experimental verifications. This work would be useful for optimizing spectral sensitivity of broadband multispectral imaging sensors or SFA sensors.

Keywords: spectral sensitivity optimization; filter selection; multispectral and hyperspectral imaging; absorption filters; imaging simulation; color reproduction; spectral reconstruction.

1. Introduction

Multispectral imaging refers to imaging with more than three to several tens of narrowband or broadband spectral channels. Since the last nineties, multispectral color imaging that spectrally sampling by broadband absorption filters has been explored in multispectral imaging community [1-6]. Broadband multispectral imaging takes advantage over narrow multispectral imaging in reconstructing smooth spectrums of imaging scene by much less number of spectral measurements, so it significantly reduces the hardware . Moreover, because the broadband techniques preserve much more spectral features such as transmission or absorption peaks than narrow multispectral imaging, broadband multispectral imaging may be more promising to reconstruct spectral information of imaging scenes in principle.

There are reports about optimizing the spectral sensitivity of multispectral camera by selecting filters among a larger number of commercial filters [3-10], varying the spectrum distribution of light source a large number of modularly LEDs 11 or properly designing of the response curve of spectral filter array (SFA) sensors [7]. Among them, selecting filter set from a large set of commercial filters is an efficient and cheaper way to set up a multispectral camera [3-10, 12].

There are two kinds of algorithms for filter selection. One is filter vector analyzing method (FVAM) ,which select filter set directly from a large number of filters assuming its performance in spectral reconstruction by minimizing spectrometric and colorimetric errors[3,7 and8]. The other is systematic recursion method (SRM), which search an optimal filter set exhaustively among all the combinations of available filter space with some spectrometric and colorimetric indices [4-6,9]. The

Preprints (www.preprints.org) | NOT PEER-REVIEWED | Posted: 29 November 2017 doi:10.20944/preprints201711.0192.v1

SRM is time-consuming because it requires large amount of data acquisition and reconstruction, while the FVAM is more straightforward due to just requiring some mathematical measurement of the filter set. Among all FVAMs, maximum linearity independence (MLI) performs better [3]. The MLI method was used to select spectral training set by Hardeberg for the first time [9], of which the insight is the transmittances matrix of the selected filter set keeping the minimum condition number. S.X. Li applied it to select filter for optimizing spectral sensitivity of multispectral camera [10]. It was verified outperforming other vector analysis methods such as maximizing orthogonality in transmittance vector space [3, 10]. However, the MLI method is limited by predefining the ℓ_2 norm of the transmittance vector of the first filter being the maximum among all those of the filters for being selected [9]. Although the traditional MLI method can assure the highest SNR (signal to noise rate) for the response of the first channel, it may not be optimal to the overall system. The insufficient of it will be discovered in this article.

To the best of our knowledge, there has been no further investigation of the MLI method in broadband filter selection. In the following, we will investigate the MLI method by varying the first filter through simulation of spectral imaging. From the best-performed filter set, the generalized characteristics of the most competent filter set is abstracted expectedly, which would help to optimizing the spectral sensitivity of broadband multispectral camera by FVAM simply.

The article is arranged as follows. We introduce MLI filter selection methods in section 2. Then experimental simulation was conducted in section 3. We abstract the features of the best-performed filter set from the results of the experimental simulation in section 4. We discuss the generalization of the results of the article in section 5.The conclusion is drawn in section 6.

2. MLI filter selection method

Contrasting to the SRM, the FVAM can be conducted by merely analyzing the features of filter transmittance vectors without considering specific linear model [1] of multispectral camera, which contains all the factors affecting the response of the camera sensor. The FVAM works well only if some mathematical measurements for spectral transmittances of corresponding filter set is competent for color reproduction or spectral reconstruction precisely, regardless of other camera parameters.[1, 7, 8]

In Ref. 1 and Ref. 8 ,several types of filters are considered to optimize the spectral sensitivity of multispectral camera by comparing their performances, including narrowband filters pairs of isolated Gaussian curve shape VS overlapped Gaussian curve shape, and both of broadband and narrowband filters selected by different selection methods of the MLI VS the *Maximum Orthogonality Method* (MOM). The results show that the overlapped filter set and filter set selected by MLI perform better. With same number of channels, broadband commercial available absorption filter sets selected by MLI performs better than the interference narrow ones. From the previous researches, we have shown that the broadband multispectral camera is more effective than narrowband ones with same number of spectral channels , and that transferring application of MLI from training set selection to filter selection has a great potential to further exploration.[1, 8, 10]

The original proposal of MLI used in multispectral color imaging is relevant to training set selection, seeking minimum numbers spectral samples in a large set of collection for the most representative subset.[9] From the perspective of linear algebra, that means the sample subset selected spans as uniformly as possible in the overall spectral space. Multispectral camera model is this:

$$[\mathrm{diag}(\mathbf{L})\cdot\mathrm{diag}(\mathbf{S})\cdot\mathbf{T}]^{\mathrm{T}}\mathbf{R}=\mathbf{C} \tag{1}$$

where the *diag(.)* denotes a diagonal matrix with elements of corresponding vector, and $[.]^{\mathrm{T}}$ denotes transpose of a matrix;

$$\mathbf{L}=[l_1 \;\cdots\; l_i \;\cdots\; l_n]^T \tag{2}$$

is a column vector of light source spectral distribution with each elements corresponding to a wavelength sample;

$$\mathbf{S}=[s_1 \;\cdots\; s_i \;\cdots\; s_n]^T \tag{3}$$

is a column vector of spectral sensitivity of imaging sensor;

$$\mathbf{T}=[\mathbf{T}_1 \ \ldots \ \mathbf{T}_i \ \ldots \ \mathbf{T}_m]=\begin{bmatrix} t_{11} & \cdots & t_{1j} & \cdots & t_{1m} \\ \vdots & \vdots & \vdots & \vdots & \vdots \\ t_{i1} & \cdots & t_{ij} & \cdots & t_{im} \\ \vdots & \vdots & \vdots & \vdots & \vdots \\ t_{n1} & \cdots & t_{nj} & \cdots & t_{nm} \end{bmatrix} \tag{4}$$

is a matrix of spectral distribution of filter transmittances with m spectral sensing channels, each column of which is a transmittance vector of a corresponding filter corresponding with n wavelength sample; $\mathbf{R}$ and $\mathbf{C}$ is column vector of reflectance and response of camera sensor respectively. Let

$$\mathbf{\Phi}=[\mathrm{diag}(\mathbf{L})\cdot\mathrm{diag}(\mathbf{S})\cdot\mathbf{T}]^{\mathrm{T}}\,, \tag{5}$$

we can see the camera model describes a linear transform from Eq.1 to Eq.5.

From the above model, $\mathbf{\Phi}$ should be an orthogonal matrix if the R can be precisely reconstructed. However, we wonder if MLI method could be an effective method for filter selection due to its independence to other camera parameters .If for sure, it can be helpful for setting up an optimized multispectral imaging camera.

The algorithm to select broadband filters by MLI is listed in Figure 1. The aim of the algorithm is to select filter sets which transmittances matrix has the minimum condition number. From Figure 1, we can see that the first selected filter is supposed to be the one which corresponding vector has the maximum ℓ_2 norm; it would lead to the highest signal to noise rate in the first channel as expected. However, there exists that the next selected filters may contain the filter with highest value of ℓ_2 norm possibly if the first filter is not the maximum $\ell_2$norm, that is to say, a highest signal to noise needed not to be gained by the first channel of the broadband multispectral camera logically. That will be verified by the following experimental simulation in section 3, where we will show that the best-performed filter set is often not the first filter with maximum ℓ_2 norm.

Task: Find filter set of M channels with minimum condition number among K (a large number) transmittances
Step 0: Collect transmittance vector sets ($\mathfrak{T}$) which comprise K transmittances;
Step 1: S=1, select transmittance vector $\mathbf{T}_1$ which ℓ_2 norm is maximum value from $\mathfrak{T}$;
Step 2: S=2, select transmittance vector $\mathbf{T}_2$ from rest vectors in $\mathfrak{T}$ which satisfies transmittance matrix, [T_1, T_2], has minimum condition number;
… …
Step M: S=M, select transmittance vector $\mathbf{T}_\mathrm{m}$ from rest vectors in $\mathfrak{T}$ which satisfies transmittance matrix, [$\mathbf{T}_1$, $\mathbf{T}_2$, ... , $\mathbf{T}_\mathrm{m}$],has minimum condition number.

Figure 1. Algorithm for select broadband filters by Maximum Linearity Independence method (MLI).

3. Experimental simulation

3.1. Datasets

In the next imaging simulation, datasets comprise transmittances of filter sets, spectral sensitivity of camera, illuminant and spectral cubic images. The filter datasets are obtained from datasheet of color filter glass of Hoya Group [12], which has 45 single filter transmittances (see Figure 2a). The physical constraints of the thickness and the transmittance of a filter must be concerned, because it would not be practical due to the thickness and transmitted energy if the number of the filters that stack up to form a filter combination is larger than 2. Therefore, let *K* denotes the number of transmittances that can be selected from the collection, which comprise single filters and combinations of two filters; and *N* denotes the number of original transmittance, then

$$K=N+\binom{N}{2}=45+\frac{45!}{2!(45-2)!}=1035\,. \tag{6}$$

The 1035 transmittances are illustrated in Figure 2b. The CIE standard illuminant D65 and camera sensitivity of Basler 302f are displayed in Figure 2c/d. The spectral data cube with

Preprints (www.preprints.org) | NOT PEER-REVIEWED | Posted: 29 November 2017 doi:10.20944/preprints201711.0192.v1

320*582=186240 voxels (the axis of "Voxels" are the position coordinates for x,y and the spectral coordinate for reflectance) ,which is formed by 24 reflectance spectrums derived from spectral measurements of 24 patches of Macbeth Color Checker; each patch of which comprises 80*97 voxels(see Figure 2g for its 2D display). All the spectral data contain 61 spectral measurements evenly sampled in wavelength range from 400-700 nm.

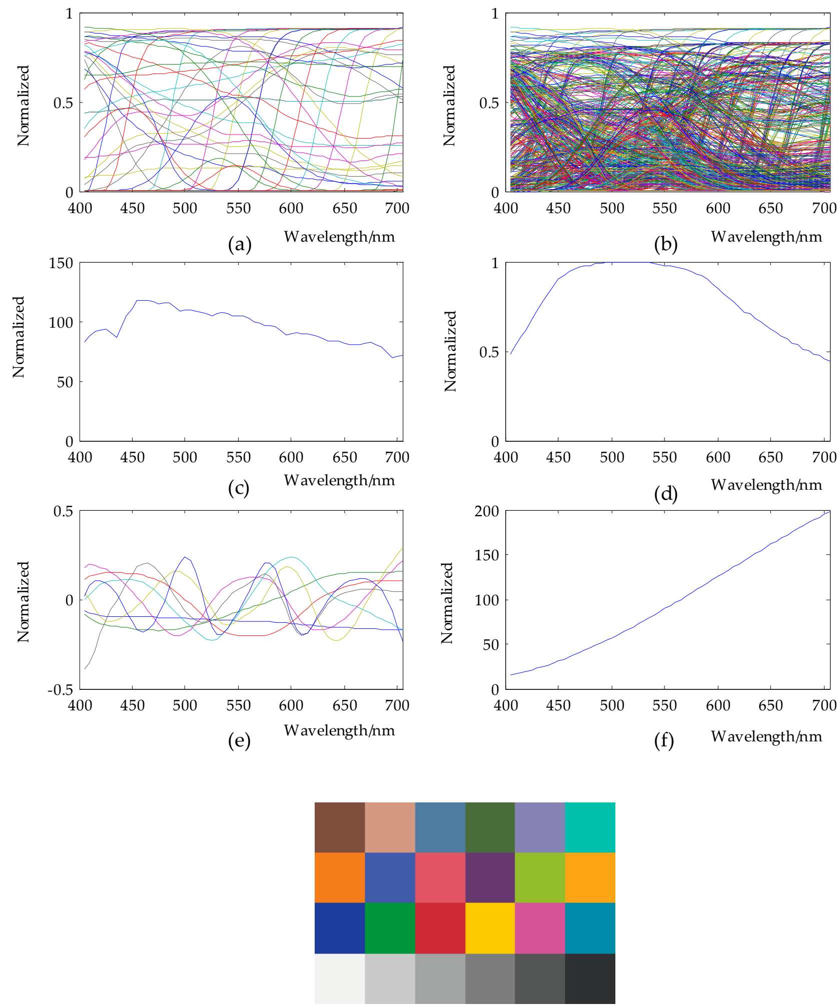

(g)

Figure 2. Visualization of data sets used for simulation. (a) Transmittances of 45 single filters. (b) All 1035 transmittances of single filters and two single filter combinations (c) Spectral distribution of CIE standard illuminant D65. (d) Camera sensitivity of Basler 302f camera sensor.(e) The first eigenvectors of spectral data of Macbeth ColorChecker.(f) Spectral distribution of CIE standard illuminant A. (g) Color display of spectral data cubic of Macbeth Color Checker.

3.2. Experimental simulation

Taking each of the 45 single filters for the first filter of every desired series of selected filter set, other filters of the intended filter set are selected from the rest of 1034 filter transmittances according to algorithm listed in Figure 1; The corresponding condition numbers of the selected filter sets are computed at the same time. In the following, the word 'No. of filter' is defined as the serial number of the single 45 filters, and the 'No. of filter set series' means a filter set series containing 4 to 8 filter channels of which the first filter is form the sequential 45 filters.

Preprints (www.preprints.org) | NOT PEER-REVIEWED | Posted: 29 November 2017 doi:10.20944/preprints201711.0192.v1

For every selected filter sets, imaging simulation below comprises three steps. Firstly, we compute the camera response image ($\mathbf{C}_{\mathrm{Re}\,sponse}$) of the original reflectance image ($\mathbf{R}_{Original}$) by adding Gaussian noise ($\mathbf{N}_{\mathrm{Gaussian}}$) according to Eq.7:

$$\mathbf{C}_{\mathrm{Re}\,sponse} = ([diag(\mathbf{L})diag(\mathbf{S})\mathbf{T}]^T \mathbf{R}_{Original})^T + \mathbf{N}_{Gaussian}. \quad \textbf{(7)}$$

Secondly, reconstructed spectral image ($\mathbf{R}_{\mathrm{Re}\,counstruct}$) is computed according to Eq.8:

$$\mathbf{R}_{\mathrm{Re}counstruct} = \psi_0 pinv(([diag(\mathbf{L})diag(\mathbf{S})\mathbf{T}]^T \mathbf{R}_{Original})^T \psi_0)\mathbf{C}_{\mathrm{Response}}\ , \quad \textbf{(8)}$$

Where *pinv(.)* denotes pseudoinverse of a matrix, and ψ_0 is a matrix which columns are the first *m* eigenvectors of the spectral reflectance of Macbeth ColorChecker (*m* is the number of channels of multispectral camera).More generally speaking, ψ_0 represents the priori information of the reflectance of the imaging scene. Maloney and Wandell used the reconstruction algorithm for the first time, into which the insight is making use of linear approximation for the reflectance by the basis vectors of the priori spectral training set [13, 14]. Finally, we evaluate the performance of spectral reconstruction relevant to the selected filter sets.

As we know, a single index is not capable of evaluating both the performance of spectral reconstruction and color reproduction in multispectral imaging. Therefore, several indices, such as PSNR, GFC, CIECDE2000 and MSE often employed in multispectral community, [2, 15-17] are adopted to appraise the performances of the selected filter sets. Considering the relatively excellent results in the following simulation computed by the expression of GFC used in literatures [16 ,17] are almost equal to 1, that is to say, losing its discrimination, the embedded Matlab function of *GoodnessofFit* are adopted to compute GFC .The formula is as follows:

$$\mathrm{GFC_{NMSE}} = 1 - \frac{\|\mathbf{R} - \widehat{\mathbf{R}}\|}{\|\mathbf{R} - mean(\widehat{\mathbf{R}})\|}, \quad (9)$$

where the cost function is normalized root mean square error (*NMSE*) of the estimated (**R**) and the reference vector ($\widehat{\mathbf{R}}$). The *NMSE* costs vary between *–Inf*. (bad fit) to *1*(perfect fit).Generally, the higher of PSNR, the more of GFC close to 1, the more of CIEDE2000 and MSE are approach to 0 , the performance of corresponding filter sets is more optimal. Note that the GFCs in this article are calculated by *Matlab* function *goodnessOfFit* (RMSE) [18].

In the simulation, we adopt five channel numbers of multispectral camera; the numbers of spectral channels are 4, 5, 6, 7 and 8 respectively. The level of additive Gaussian noise denoted by *SNR* (signal to noise rate) is varied by the ten noise levels in *DB*s, where *SNR*∈[∞, 50, 47, 43, 40, 37, 33, 30, 27, 23].The relationship of SNR and the noise variance is defined by

$$\sigma = 10^{-\frac{\mathrm{SNR}}{10}}, \quad (10)$$

The noise is added by the imnoise Matlab function to the response image $\mathbf{C}_{\mathrm{Re}\,sponse}$ described in Eq.7.

4. Results and analysis

4.1 Data reduction

From the simulation, we acquired 2250 groups of results for investigation. Each of them is relevant to a number of channels and a noise levels, and contains four evaluation indices that are PNSR, GFC, CIEDE2000 and MSE. From the results, the performances of the filter sets are generally consistent with each other in that the higher SNR of noise level and the channel number are the better performance of the filter set series is. We can take the GFCs of the first four filter sets for example (see Figure 3). From Figure 3, we can see the performances of the filter sets with different series numbers differ from each other distinctly, and the general trends of performance when varying the number of channels and noise levels. However, we can hardly recognize the specific best-performed filter set among so much of items. It is necessary to find a measurement to evaluate the performance of the filter series quantitatively.

doi:10.20944/preprints201711.0192.v1

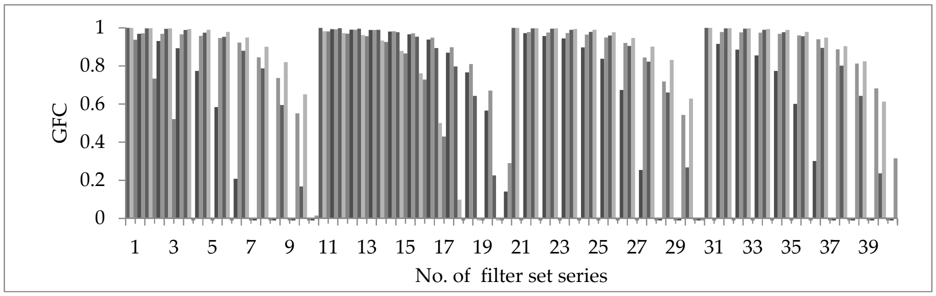

Figure 3. The GFCs of the first four filter series (only positive values are displayed for clarity),where each of the four groups of stems presents the performance of the corresponding filter sets under ten noise levels and four number of channels. From the left to the right of each group, ten clusters of stems illustrate the GFCs in terms of different noise levels in descending order; each of the clusters contains five numbers of the channels of multispectral camera. The numbers of channels are 8,7,6,5 and 4 from the left to the right.

We have computed the mean, maximum and minimum of all the 50 datasets relevant to each one filter set series. Fig.4 shows the overall performances of the 45 series of filter sets in terms of GFC, where the upper round marker denotes the maximum value; the middle square denotes the mean; and the lower round denotes the minimum (some of the minimums with negative value less than -2 are not displayed). We can see which series of filter sets performance better intuitively. So does the filter sets with specific channels, as we can see that in Fig. 5. Those in terms of other evaluation indices have similar characteristics, which are omitted here for clarity.

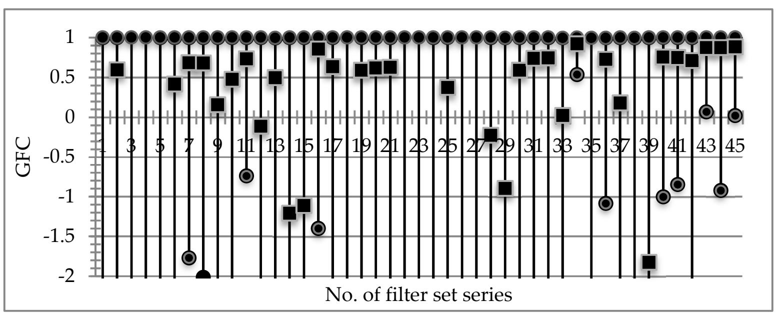

Figure 4. Overall performances of the 45 series of filter sets in terms of GFC.

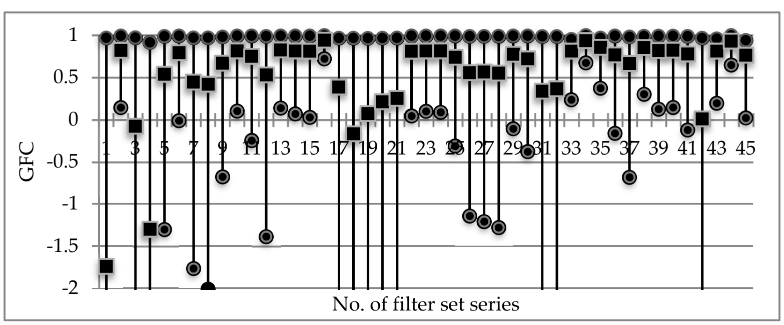

Figure 5. Overall performances of the 45 series of filter sets for 6 channels in terms of GFC.

As we have known, we cannot tell which filter set performs better by only one index. However, if a filter set has the maximum frequency out of the best-performance filter sets collection in terms of different indices, we can reasonably conclude that the filter set is the best one. Therefore, we collect the top best-performed filter sets (for 20% in this article) in terms of the entire four indices to find the largest frequency of a filter set getting involved.

Preprints (www.preprints.org) | NOT PEER-REVIEWED | Posted: 29 November 2017 doi:10.20944/preprints201711.0192.v1

4.2 Data sorting and the best-performed selection with overall channels

Table.1 Statistics of the top 20% best-performed filter set series.

PSNR				GFC			
No.	**H-mean**	**No.**	**H-min**	**No.**	**H-mean**	**No.**	**H-min**
45	37.68	45	25.10	34	0.9215	34	0.5347
44	35.87	43	21.73	45	0.8829	43	0.0649
43	35.74	11	20.54	43	0.8728	45	0.0193
11	35.55	36	20.22	44	0.8722	11	-0.7395
36	34.78	2	18.56	16	0.8536	41	-0.8475
12	34.75	7	18.04	40	0.7544	44	-0.9224
13	34.49	13	18.00	41	0.7484	40	-1.0018
28	34.34	8	17.95	32	0.7437	36	-1.0851
40	33.83	41	17.87	31	0.7364	16	-1.3993
MSE				**CIEDE2000**			
Series No.	L-mean	Series No.	L-min	Series No.	L-mean	Series No.	L-min
45	2.20E-03	33	5.68E-05	45	4.67	42	0.09
43	4.43E-03	38	6.27E-05	43	5.13	35	0.10
11	5.06E-03	35	6.33E-05	38	6.88	38	0.11
36	6.14E-03	42	6.33E-05	13	6.94	33	0.13
44	7.84E-03	45	6.40E-05	44	6.98	26	0.14
12	8.22E-03	3	6.41E-05	11	7.04	27	0.14
13	8.69E-03	27	6.48E-05	36	7.15	1	0.14
28	9.66E-03	26	6.49E-05	12	7.67	5	0.15
2	1.08E-02	5	6.52E-05	28	7.77	3	0.15

Table 1 list the results of the top 20% best-performed filter sets in terms of PSNR, GFC, MSE,CIEDE2000, where the data of PSNR and GFC are sorted in descend way, and those of MSE and CIEDE2000 are sorted in ascend way. All the data are derived from their corresponding averages of each index, which include those of all the 10 noise levels and all the channel numbers of the filter set series. In table 1, the No. denotes the No. of filter set series; H-mean denotes descend order of the means; H-min denotes descend order of the minimums; L-mean denotes ascend order of the means and L-min denotes ascend order of the minimums. From table 1, we can see the order of the sorted data relevant to each specific filter set series is not consistent; however, there are some appearing frequently. For convenient, we count the frequency of the each emerged filter set series, the results are demonstrated in Figure 6 (a).From Figure 6 (a),we can see the No.45 have the most frequency in the nine best-performed results, and the No.11,43,44 rank the second place. Moreover, we can see from table 1 and Fig. 6 (a) that the No.2 filter set series in which the transmittance vector of the first filter has the maximum ℓ_2 norm is not the best-performed filter set series.

Another method to decide explicitly which filter set being more optimal is score ranking method. The score ranking method is designed like this: Let the first filter series in table 1 having the highest score of 9, the second having 8 and so on, then we can get the cumulated scores of the filter sets series. The results are figured in Fig. 6 (b).From Fig. 6(b), we can see that the above the No.11,43 and 44, which are ranked in the same second place in Fig.6(a) , can be discriminated numerically.

Preprints (www.preprints.org) | NOT PEER-REVIEWED | Posted: 29 November 2017 doi:10.20944/preprints201711.0192.v1

Especially, if there is not just one filter set series sharing a same maximum frequency, the score ranking method may be irreplaceable.

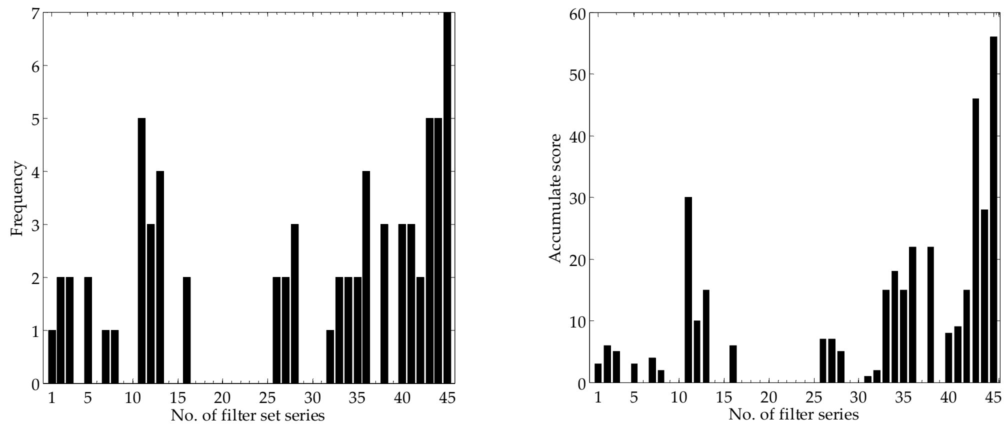

(a) **(b)**

Figure.6 Statistics of the best-performed filter set series. (a) Frequency ; (b) Accumulative scores.

4.3 Best-performed selection with single channel number

We have computed statistics of the top 20% best-performed filter sets with 4-8 channels respectively in terms of PSNR, GFC, MSE, and CIEDE2000.All the data are derived from their corresponding averages of each index, which comprise those with all the 10 noise levels. In this section, we give the performances of filter sets in terms of different channel numbers. The data are processed by score ranking method in the same way as in section 4.2, and the results together with those of the overall channels in section 4.2 are listed in table 2, where the best-performed filter set series and the highest cumulative scores are printed in bold.

Table 2. Accumulative scores of the nine best-performed filter sets or series with D65.

No.	**scores**	**No.**	**scores**	**No.**	**scores**	**No.**	**scores**	**No.**	**scores**	**No.**	**scores**
4 channels		**5 channels**		**6 channels**		**7 channels**		**8 channels**		**all channels**	
45	43	**38**	48	**44**	**57**	**44**	50	**45**	**57**	**45**	56
43	42	16	42	45	41	35	47	34	31	43	46
38	33	44	39	11	37	38	38	12	31	11	30
16	31	45	31	16	36	45	32	28	29	44	28
36	30	13	30	40	30	43	27	33	28	38	22
13	27	35	20	43	27	34	22	43	28	36	22
29	23	34	18	42	21	33	18	13	24	34	18
35	23	40	14	33	19	25	16	27	23	42	15
44	16	43	13	34	16	27	14	42	15	35	15

4.4 Comparison with the performance of best selection and the past selection

We have computed the ℓ_2 norms for the transmittance vectors of the 45 filters, and revealed that that of the No.2 filter was the maximum. From table 2, we can see the No.44 and 45 filter set series have same maximum accumulative scores (57). But the No. 44 filter set series has the maximum accumulative scores and a smaller number of channels (6 channels) comparing with those

Preprints (www.preprints.org) | NOT PEER-REVIEWED | Posted: 29 November 2017 doi:10.20944/preprints201711.0192.v1

of the No.45 filter set series (8 channels). Therefore, we display the results of the No.44 and No.2 filter set series with 6 channels in table 3 for comparison. From table 3, we can see the performance of the No.44 is greatly improved comparing to the No.2 .The same conclusion can also be made from table 2, in which all the filter set series listed outperform the No.2 filter set series.

Table 3. Performance of the best-performed filter set and the past selection one for 6 channels.

Indices	PSNR		GFC		MSE		DE2000	
No.	44	2	44	2	44	2	44	2
Average	38.434	32.11	0.9318	0.1617	2.39E-03	1.72E-02	4.13	10.494

4.5 Presentation of the best performed MLI filter sets with different noise

From table 2, we can see the best filter set selected by MLI, however the specific performance of those filter sets at each noise level may be meaningful to practical application. Table 4 lists the results of performance for the filter sets. From table 4, we can see the performance of each best filter set at specific noise level, which can be a quantitative reference for practical applications.

Table.4 Performances of the best filter sets.

Noise /DB	∞	50	40	37	33	30	27	23
N0.45/4 channels								
PSNR/DB	42.33	41.36	38.95	37.78	35.76	33.82	31.68	28.50
GFC	0.9835	0.9823	0.9704	0.9587	0.9245	0.8689	0.7778	0.5422
MSE	6.07E-04	6.17E-04	7.11E-04	8.19E-04	1.13E-03	1.64E-03	2.64E-03	5.47E-03
DE2000	1.09	1.46	2.83	3.72	5.48	7.29	9.73	13.61
N0.38/5 channels								
PSNR/DB	43.46	42.41	39.13	37.35	34.40	31.96	29.29	25.63
GFC	0.9900	0.9880	0.9707	0.9509	0.8998	0.8159	0.6679	0.3004
MSE	3.51E-04	3.74E-04	5.85E-04	8.02E-04	1.49E-03	2.60E-03	4.82E-03	1.11E-02
DE2000	0.49	0.96	2.46	3.35	5.15	6.92	9.18	13.22
No.44/6channels								
PSNR/DB	49.40	45.72	40.56	38.33	35.12	32.46	29.69	26.11
GFC	0.9994	0.9984	0.9897	0.9799	0.9522	0.9139	0.8371	0.6556
MSE	2.54E-04	2.80E-04	5.07E-04	7.69E-04	1.52E-03	2.77E-03	5.19E-03	1.19E-02
DE2000	0.70	1.05	2.30	3.07	4.64	6.22	8.38	11.94
No.44/7channels								
PSNR/DB	50.38	46.88	40.92	38.45	34.89	32.11	29.29	25.56
GFC	0.9993	0.9984	0.9896	0.9783	0.9500	0.9071	0.8437	0.6634
MSE	1.22E-04	1.52E-04	4.22E-04	7.21E-04	1.64E-03	3.10E-03	5.93E-03	1.40E-02
DE2000	0.42	0.81	2.06	2.77	4.27	5.75	7.67	11.02
No.45/8channels								
PSNR/DB	52.92	47.91	40.94	38.32	34.52	31.69	28.85	25.10
GFC	0.9996	0.9982	0.9857	0.9724	0.9331	0.8732	0.7764	0.5173
MSE	6.40E-05	9.35E-05	3.56E-04	6.48E-04	1.54E-03	2.96E-03	5.73E-03	1.38E-02
DE2000	0.25	0.89	2.47	3.41	5.22	7.02	9.43	13.29

Preprints (www.preprints.org) | NOT PEER-REVIEWED | Posted: 29 November 2017 doi:10.20944/preprints201711.0192.v1

4.6 Characteristics of the best-performed MLI filter sets

The condition numbers of the best-performed filter set series and those of No.2 series are listed in table 5, where the figures printed in bold are condition number of the filter sets with the best-performed channels. The condition numbers of the entire filter set series are displayed in Fig.7 by radar charts.

From table 5, the condition numbers of the best filter sets is less than 4, although the condition numbers are not always the minimum for the best-performed filter set. From Fig7, we can see the condition numbers listed in table 5 are one of the several smallest among all the condition numbers. Therefore, it indicates that minimizing the condition number of a filter set is an essential precondition for optimizing the sensitivity of broadband camera, and the best-performed filter set must be the one with a smaller condition number than most of the condition numbers of the others.

Table 5. Condition numbers of the best-performed filter set and the conventional selection.

Channels	No.45	No.38	No.44	No.2
4	**1.45**	1.65	1.37	5.84
5	2.11	**2.56**	1.63	6.65
6	2.55	3.21	**2.31**	9.74
7	3.04	3.91	**3.10**	12.01
8	**3.62**	92.35	20.34	13.99

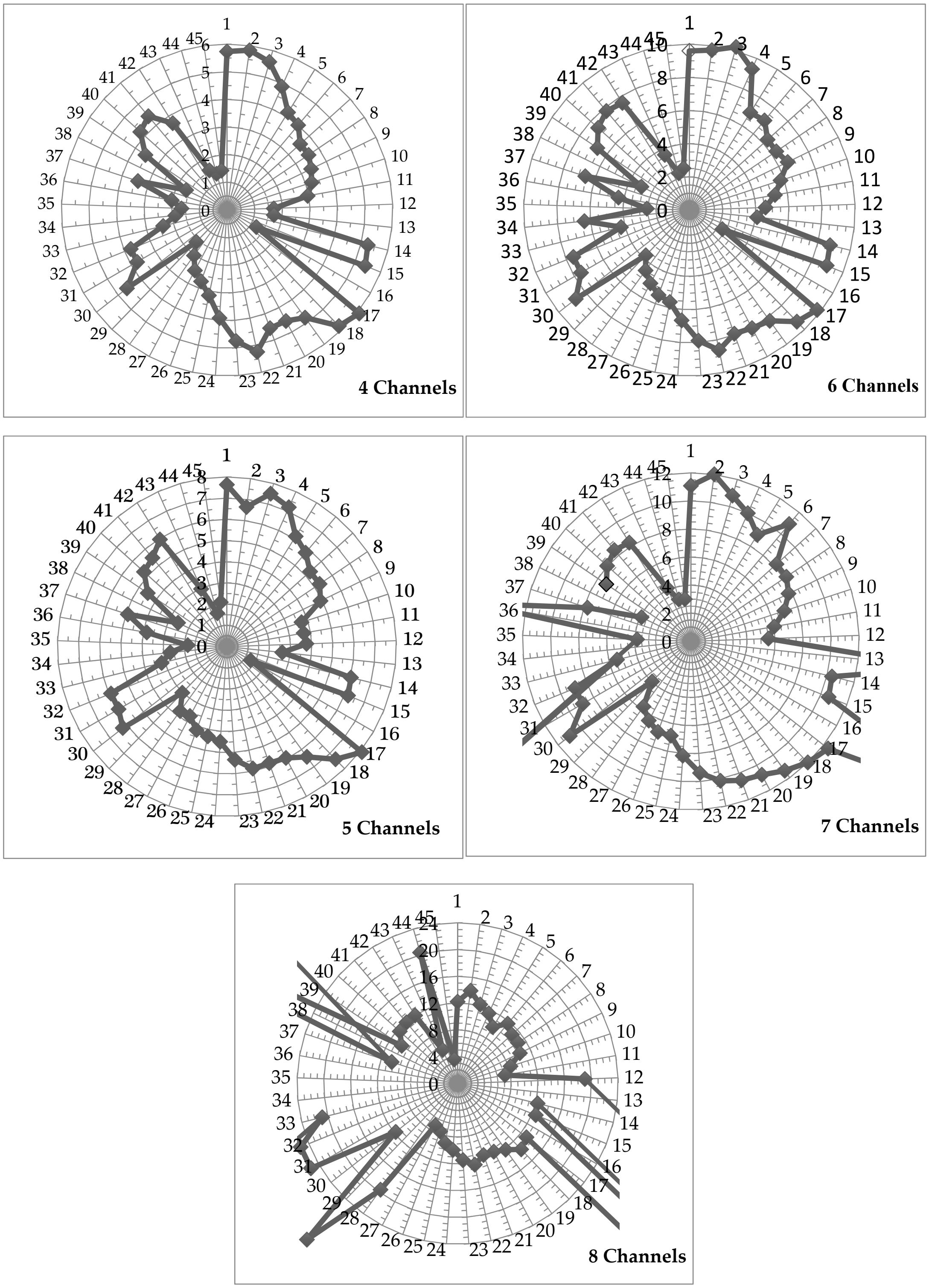

Figure 7. The condition numbers versus the corresponding filter sets and channel numbers. The radical coordinates denote condition numbers and the angular coordinates denote the No. of the filter sets, therefore the square markers denote the position of the corresponding filter sets. In the radar charts for 7 and 8 channels, some of the condition numbers cannot be seen because they are too large to be displayed and we are more concern with the smaller ones.

Preprints (www.preprints.org) | NOT PEER-REVIEWED | Posted: 29 November 2017 doi:10.20944/preprints201711.0192.v1

For further investigation, the transmittances of the best-performed filter sets in table 4 are graphed in Fig. 8, where the first filter of the filter sets is graphed in bold line with round markers. Comparing to No. 2, we can see that the first filter of the best set has a distinct transmittance peak and the peaks of the sequential filters distribute almost evenly in the wavelength range. Comparing No.38 and No.45 or N.44 when the No. of channels equals 5, we can see that the best filter set (No.38) has higher transmittances and more overlaps than the first five channels of No.44 or No.45. Similarly, we can see the consistent geometric distribution of the first 4 filters of best performed No.45 filter set versus that of the No.44.Especially we can see there is a large notch in wavelength from 580nm to 630nm or so, which may be the cause of No.44 has worse performance than No.45 at the channels number being equal to 4.

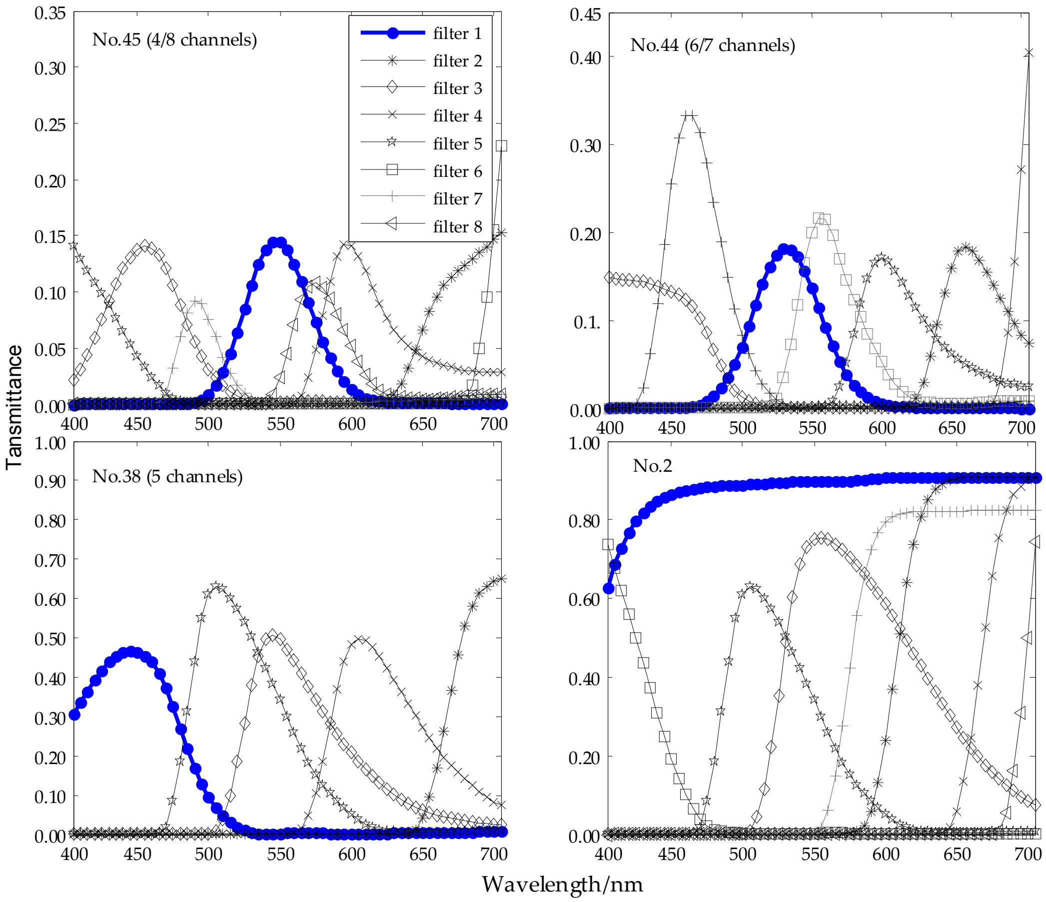

Figure 8. Transmittances of the best-performed filter sets (from No.45, 44 and 38) and the filter set series with maximum ℓ_2 norm first filter (No.2).

5. Discussion

5.1 General applicability of the MLI method with varying imaging parameters

We have revealed the characteristics of the best-performed filter sets from above simulation; however, we want to know its general applicability when changing the camera parameters, especially varying the illuminant. Among the parameters related in section 2, the imaging illuminant is varying easily under real condition, for example, lighting uncontrollable outdoor imaging. Therefore, we make another simulation with the CIE standard A illuminant graphed in Fig.2f. The results correspond to table 2 are listed in table 6,which display the accumulative scores

Preprints (www.preprints.org) | NOT PEER-REVIEWED | Posted: 29 November 2017 doi:10.20944/preprints201711.0192.v1

of the first four best-performed filter sets or series with A illuminant; and the performance of the best-performed filters in A illuminant are listed in table 7.

Table 6. Accumulative scores of the four best-performed filter sets or series with A illuminant.

No.	scores	No.	scores	No.	scores	No.	scores	No.	scores
4 channels		5 channels		6 channels		7 channels		8 channels	
45	43	**16**	50	**44**	52	**44**	50	**45**	57
43	40	38	42	45	43	35	46	34	31
16	36	45	39	16	38	38	37	12	31
38	33	44	37	34	31	45	31	28	29

Table.7 Performances with A illuminant of the best filter sets.

Noise /DB	**∞**	**50**	**40**	**37**	**33**	**30**	**27**	**23**
N0.45/4 channels								
PSNR/DB	41.97	40.97	38.48	37.16	35.07	33.09	30.96	27.67
GFC	0.9867	0.9855	0.9737	0.9612	0.9216	0.8731	0.7819	0.5020
MSE	6.63E-04	6.76E-04	7.94E-04	9.30E-04	1.32E-03	1.97E-03	3.21E-03	6.81E-03
DE2000	0.65	1.02	2.42	3.28	4.52	5.68	7.00	8.85
N0.16/5 channels								
PSNR/DB	43.46	42.41	39.13	37.35	34.4	31.96	29.29	25.63
GFC	0.9989	0.9981	0.9905	0.9824	0.9584	0.9259	0.8625	0.6799
MSE	6.32E-04	6.52E-04	8.25E-04	1.01E-03	1.57E-03	2.49E-03	4.30E-03	9.44E-03
DE2000	0.93	3.45	8.42	10.18	13.15	14.49	15.59	16.00
No.44/6channels								
PSNR/DB	40.86929	40.40447	38.37405	37.17598	34.85175	32.74033	30.30314	26.85012
GFC	0.9994	0.9984	0.9896	0.9799	0.9487	0.9140	0.8413	0.6685
MSE	3.12E-04	3.52E-04	7.07E-04	1.08E-03	2.25E-03	4.06E-03	7.81E-03	1.84E-02
DE2000	0.66	0.93	2.15	2.94	4.04	5.20	6.47	8.31
No.44/7channels								
PSNR/DB	49.84912	45.72807	39.52636	37.02057	33.49637	30.69482	27.7842	24.08812
GFC	0.9994	0.9985	0.9896	0.9804	0.9529	0.9099	0.8386	0.6561
MSE	1.38E-04	1.86E-04	6.01E-04	1.08E-03	2.47E-03	4.77E-03	9.33E-03	2.21E-02
DE2000	0.43	0.80	2.04	2.73	3.82	4.79	6.04	7.59
No.45/8channels								
PSNR/DB	53.17	47.32	39.78	37.13	33.32	30.42	27.56	23.71
GFC	0.9996	0.9982	0.9845	0.9700	0.9245	0.8718	0.7596	0.4668
MSE	6.68E-05	1.08E-04	4.79E-04	8.76E-04	2.10E-03	4.08E-03	7.96E-03	1.93E-02
DE2000	0.41	1.00	2.54	3.28	4.65	5.90	7.33	9.44

Comparing to table 4, the best-performed filter set in table 6 are almost the same at the number of channels equaling to 4, 6, 7 and 8, although the different light source was used. An exception is the No.16 filter set at the number channels equals 5. The transmittance curves of No.16 filter series are displayed in Fig. 9, and the condition numbers of them are listed in table

 doi:10.20944/preprints201711.0192.v1

8.Comparing the curves from Fig. 9 with those of Fig. 8, the same conclusions can be made with No.16 as that of N0.38, and so do the condition numbers in table 7. Form the ranking cumulate score table (see table 8), in fact, we can see No.38 is the closest 5 channels filter set just behind the best-performed, No.16 filter set. The performance is slightly better in A illuminant than that of D65 comparing table 2 to table 8, however the best performed filter are still those with smaller condition numbers and characteristics of curve shapes . The facts that the best-performed filter sets with CIE A illuminate support our conclusion about the criterions to the best-performed filter sets derived from those with CIE D65 illuminate. In other word, the criterions to select filter set to optimizing the spectral sensitivity of broadband camera is independent to the imaging parameter, light source, which illuminate the imaging scene.

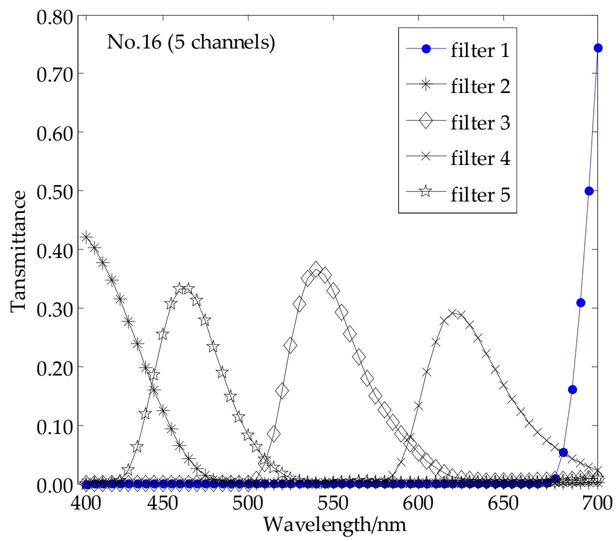

Figure 9. Transmittances of the best-performed filter set, No.16 (5).

Other imaging parameters may be changed for similar simulation such as varying the camera spectral sensitivity function and the spectral imaging scene; unfortunately, there remains no more necessary energy to do that. The generalization of the conclusions about the criterion of the competent filter set selected by MLI would be justified by the simulations with varying the light source above.

5.2 Two intuitive steps for MLI method to selecting filter sets

From the simulation above, we can select the best filter set for optimizing the sensitivity of broadband multispectral camera by the characteristics such as the condition number and the geometric distribution of the transmittance curves. However, the methodology is intuitive and still difficult to operate in practice. The reasons lie in two aspects.

The one is that the best-performed filter set is not always the one with the smallest condition number as it can been seen in table 5 and from comparison between table 2, table 7 and Fig.7.The other is that the characteristics of the transmittance curves of the filter set is too intuitive to be handled quantitatively. Therefore, we recommend two steps to obstacle the problem.

The first step is to select a subset of the filter sets with smaller condition number from the entire filter sets. Comparing table 2 and table 7 to Fig.7, we can see the best-performed filter set stays among several filter sets with the smallest condition numbers. Table 8 list the ordinal numbers of condition number sorted from small to large among 45 corresponding condition numbers for the best-performed filter sets. From table 8 we can see that the condition numbers of the best-performed filter sets are almost the closest to the most smallest; the farthest is condition numbers of No. 38 filter set, of which the ordinal number is 5 in all the 45 filter sets. Namely, if the

Preprints (www.preprints.org) | NOT PEER-REVIEWED | Posted: 29 November 2017 doi:10.20944/preprints201711.0192.v1

subset of filter sets is composed by the 5 filter sets with the smallest condition number, we can decide the best-performed filter set is in it.

The second step is to select a filter set among the subset in terms of the geometric distribution of its transmittance curves or by a few experimental explorations. The geometric distribution of the transmittance curves of a best-performed filter sets related above would give an intuitive criterion to identify the best-performed filter set from the subset conveniently, otherwise experimental explorations can be conducted with every filter set in the subset to pick out the best-performed filter set according the experimental results. Because of the number of the filter sets in the subset is less than five according to the results of this article, it would also be an efficient way to select the best-performed filter set in the subset .

Table 8. Ordinal number of the condition numbers of the best-performed filter sets with different illuminant.

Channels	4	5	6	7	8
Filter No.	45	38	44	44	45
D65	3	5	2	2	1
Filter No.	45	16	44	44	45
A	3	1	2	2	1

So far, we have investigated selecting broadband filter set from a large number of commercial filters to optimizing the spectral sensitivity of broadband multispectral imaging camera by imaging simulation. From the results of the simulation, we found the remarkable characteristics of the best-performed filter set. Besides smaller condition number of the best-performed filter set, the geometric features of it comprise the distinct peak of the transmittance of the first filter, the generally uniform distributing of the peaks of the transmittance curve of the filters and the substantial overlapping of the transmittance curves with those of the adjacent filer sets.

It is worth noting that one reason of only selecting 45 single filters from1035 filters as the first filter is to reduce the calculating pressure, and the other is that the single filter is easier to implement than the combinations in practice application. Other 990 filters achieved by combination of two single filters may be serving as the first filter; it would produce more filter set series for selected by the MLI method related above, therefore it would lead the spectral sensitivity of broadband multispectral camera to be more optimizing.

Although derived by the simulation with glass transmittance filters illustrated in Fig. 1a, the results of this paper can applied to other types of filters, for example, the transmittance design of SFA (spectral filter array) multispectral system. We can see it as an experimental explanation to answer why the spectral transmittances would make it work well for SFA multispectral system.[7, 19]

6. Conclusions

Vector analysis method for selecting broadband filters is an efficient way to optimal spectral sensitivity of multispectral camera without time-consuming imaging simulation or experiments from commercial filters. In this paper, we introduced the background strategy and the algorithm of the MLI filter selection method; we questioned the reason why the first filter is selected by the maximum ℓ_2 norm of its transmittance vector. Then we conducted an exhaustive simulation searching for the best-performed filter set based on MLI by varying the first filter selected in turn from the entire single-chip broadband filter collection. From the results of the simulation, we found that there are filter sets selected by MLI outperforming the filter set selected by MLI with maximum ℓ_2 norm filter serving as the first selected filter as expected. The optimal filter set has distinct characteristics of smaller condition number and remarkable geometry characteristics, such as distinct peak of the transmittance of the first filter, generally uniform distributing of the peaks of the transmittance curve of the filters, and substantial overlapping of the transmittance curves with those

Preprints (www.preprints.org) | NOT PEER-REVIEWED | Posted: 29 November 2017 doi:10.20944/preprints201711.0192.v1

of the adjacent filer sets. The characteristics can serve as an intuitive criterion of filter vector analyzing method for optimizing the broadband multispectral imaging sensors or the spectral sensitivity of SFA sensors due to considering the variation of the noise conditions in the experimental simulation. As a future work, the characteristics of the best-performed filter set selected by MLI vector analyzing method may be modeled mathematically such that a more precisely described criterion for broadband filter selection by MLI would be put forward; furthermore, the criterion would be investigated with actual experiments using real camera(s), tested in an actual scenario.

Acknowledgments: The work was supported by the Talent Introduction research foundation of Binzhou University (No.801001021616), the Dual Targets for regional and industrial research foundation of Binzhou University (No.BZXYHZ20161008) and the Key Project Foundation of High Definition Satellite of CCRSDA.

Author Contributions: Sui-Xian Li wrote the manuscript and was responsible for the research design, data collection, and analysis. A-Qi Xu，Li-Yan Zhang and Jun Lin assisted in methodology development and research design and participated in the writing of manuscript and its revision.

Conflicts of Interest: The authors declare no conflict of interest.

References

1. Li Suixian; Zhang Liyan. Optimal Sensitivity Design of Multispectral Camera Via Broadband Absorption Filters Based on Compressed Sensing. Springer Proceedings in Physics, vol. 192, 3rd International Symposium of Space Optical Instruments and Applications, Beijing, China, Sep. 26-29,2016;Urbach H., Zhang G. ,Eds. Springer, Cham, Switzerland,2017 .(DOI:10.1007/978-3-319-49184-4_33)
2. Shrestha, R; J. Y. Hardeberg. Spectrogenic imaging: a novel approach to multispectral imaging in an uncontrolled environment. Opt. Express **2014**, 22(8),pp.9123-33.
3. J. Y. Hardeberg. Filter Selection for Multispectral Color Image Acquisition. ImagingSci.Techn.**2004**，48(2),pp.177-182.
4. F. H. Imai; S. Quan; M. R. Rosen; R. S. Berns. Digital camera filter design for colorimetric and spectral accuracy. Proc. of 3rd International Conference on Multispectral Color Science,,pp13-16,University of Joensuu,Finland,2001.
5. D. Y. Ng; J. P. Allebach. A subspace matching color filter design methodology for a multispectral imaging system. IEEE T Image Process,2006,15(9), pp.2631– 2643.
6. S. Quan; N. Ohta; N. Katoh. Optimization of camera spectral sensitivities. Proc. of the IS&T and SID 8th Color Imaging Conference, pp. 273-277, IS&T, Springfield, VA, 2000.
7. P. L. Vora; H. J. Trussell. Measure of goodness of a set of color-scanning filters. J. Opt. Soc. Am. A,1993, 10(7), pp.1499-1503.
8. S. X. Li; N. F. Liao; Y. N. Sun. Optimal Sensitivity of Multispectral imaging system based on PCA, Opto-Electronic Engineering (published in Chinese),2006,33(3),pp.127-132.
9. J. Y.Hardeberg. Acquisition and Reproduction of Color Image: Colorimetric and Multispectral Approaches, ISBN: 1-58112-135-0, Http://www.dissertation.com,USA,2001.
10. Li Suixian. Several problems research of multispectral imaging, Dissertation for PHD degree (published in Chinese),Beijing institute of technology,2007.
11. R.Shrestha;J.Y.Hardeberg. Multispectral imaging using LED illumination and an RGB camera.21st Color and Imaging Conference Final Program and Proceedings, Society for Imaging Science and Technology,pp.8-13,2013.
12. URL:http://www.hoyaoptics.com/color_filter.Hoyo corporation USA optical division.
13. L. T. Maloney; and B. A. Wandell. Color constancy: a method for recovering surface spectral reflectance.J. Opt. Soc. Am. A,Optics & Image Science , 1986,3(1), pp.29-33.
14. M. A. López-Alvarez, J. Hernández-Andrés, E. M. Valero, and J. Romero, "Selecting algorithms, sensors, and linear bases for optimum spectral recovery of skylight," J. Opt. Soc. Am. A,2007,24(4),, pp.942-956.
15. Xun Cao; Tao Yue; Xing Lin; Stephen Lin;Xin Yuan; Qionghai Dai; Lawrence Carin; David J. Brady' Computational Snapshot Multispectral Cameras: Toward dynamic capture of the spectral world. IEEE Signal Proc. Mag.,2016,33(5), pp.95-108.

 doi:10.20944/preprints201711.0192.v1

16. Huiliang Shen;,Jianfan Yao; Chunguang Li; Xin Du;Sijie Shao ; John H. Xin. Channel selection for multispectral color imaging using binary differential evolution. Applied Optics ,2014,53(4), pp.634-642.
17. Raju Shrestha; Jon Yngve Hardeberg. Spectrogenic imaging: A novel approach to multispectral imaging in an uncontrolled environment. Opt. Express,2014, 22(8) , pp.9123-9133.
18. MathWorks. Available online:https://cn.mathworks.com/help/ident/ref/goodnessoffit.html (accessed on 20 June 2017)
19. Jean-Baptiste T; Pierre-Jean L; Pierre G and Cedric C.. Spectral Characterization of a Prototype SFA Camera for Joint Visible and NIR Acquisition, Sensors,2016, 16, pp.993(1-19). (DOI:10.3390/s16070993)